METHODS AND SUPPLEMENTARY INFORMATION FOR "IMPLICATIONS FOR CLIMATE SENSITIVITY FROM THE RESPONSE TO INDIVIDUAL FORCINGS"

KATE MARVEL, GAVIN A. SCHMIDT, RON L. MILLER, AND LARISSA S. NAZARENKO

1. Simulations

We use a large suite of historical simulations from the GISS-E2-R model[12] with multiple subsets of relevant forcings as archived in the CMIP5 database. Specifically, we use a 6-member ensemble of simulations with "historical" forcings including well-mixed greenhouse gases, anthropogenic aerosols, land use/land cover change, ozone changes, and volcanic and solar forcing[8]. Additionally, we use 5-member ensembles with each of the forcings run separately ("historicalMisc" simulations).

The model consists of GISS ModelE2 for the atmosphere coupled to the Russell ocean model. All simulations use physics version 1 (Non-Interactive atmospheric composition - NINT), in which aerosols and ozone are read in via pre-computed transient aerosol and ozone fields. The aerosol indirect effect is parameterized. Further information on the model configuration and specific experiments can be found online at `http://data.giss.nasa.gov/modelforce/Marvel_etal2015.html`.

2. Perfect Model Framework

The GISS model output provides all the diagnostics necessary to determine the transient climate response and equilibrium climate sensitivity for each single-forcing ensemble and for the "historical" ensemble using previously established methodologies. Surface air temperatures and ocean potential temperatures are available as standard CMIP5 output. Because radiative forcing calculations were not required in CMIP5, we have made iRF time series and ERF values for the GISS model simulations available on the GISS website at `http://data.giss.nasa.gov/modelforce/`.

In this section, we describe the calculations performed in order to obtain ΔT, ΔF, and ΔQ from the GISS-E2-R simulations. The relevant time series and values are plotted in Figure S1, and described in further detail below.

2.1. **Instantaneous radiative forcing (iRF) definition.** We calculate the TOA radiative forcings associated with each climate driver using a radiation-only calculation for each year between 1851 and 2005 with the driver changing, but with all other variables set at pre-industrial (1850) values. In each case, we approximate the effect of rapid stratospheric adjustment by evaluating the forcing at the tropopause instead of top of atmosphere [6, 8,]. The 10-year running means of iRF for each single-forcing ensemble are plotted as dashed lines in Figure S1(a)-(g) .

2.2. **Effective radiative forcing (ERF) definition.** The effective radiative forcing is calculated from climate model runs in which the forcing is held constant at year 2000 values and SSTs are fixed at their 1850 values. Following [4], we define effective radiative forcing as

$$ERF = F_o + \Delta T_a/\lambda$$

where F_o is the flux change at the top of the atmosphere, ΔT_a the global surface air temperature change with SSTs fixed at pre-industrial values (i.e., as they were in 1850), and λ taken from previously published GISS-E2-R simulations . This technically assumes unit efficacy for all forcings, but the response term $\Delta T_a/\lambda$ is in general small compared to the TOA flux change. All values are ten-year means. When ERF is used, TCR and ECS are calculated as the quotient of 1996–2005 average ΔT and year-2000 ERF and year-2000 ERF minus 1996–2005 trends in ocean heat uptake, respectively. The calculated ERF 10-year averages centered on the year 2000 are shown as unfilled dots in Figure S1(a)-(g). We obtain similar results when ERF is calculated using 30-year averages.

2.3. **Model ocean heat content.** As in Palmer et al.[11], we calculate the ocean heat content (OHC) for every simulation using

$$\Phi = \sum_{i,j,k} \rho C \theta_{i,j,k} A_{i,j} dz_k \tag{1}$$

where $\rho = 3985$ J kg^{-1} K^{-1} is the specific heat content, $\rho = 1025$ kg m^{-3} the density of seawater, θ is the annual mean ocean potential temperature, and $A_{i,j}$ the area of the grid cell. Because the Russell ocean model is mass-conserving, we multiply the area by the varying vertical layer thickness dz.

The single-forcing experiments are spun off from a long pre-industrial control run, with the first ensemble member branching after 3981 years of integration and subsequent members branching at 20-year intervals. To account for a small residual control run drift, we subtract the linear trend in the relevant control run time period from each ensemble member, thereby calculating an anomaly time series relative to the pre-industrial period. Alternate methods to assess drift (such as a loess fit) make no significant difference to our results. We estimate the decadal rate of ocean heat uptake by calculating the best-fit linear trend to 10-year segments of OHC. Ensemble average ocean heat uptake rates for each single-forcing simulation are shown in Figure S1(a)-(g) as solid lines.

2.4. **Temperature anomalies.** For each simulation, we calculate global-average, annual-average temperature anomalies with respect to pre-industrial control averages. Any temperature drift in the pre-industrial control run is removed using the same procedure as used for ocean heat content. These time series are plotted in Figure S1(h).

2.5. **Calculating ECS and TCR.** As discussed in the main text, we calculate ECS and TCR using

$$\Delta F = \lambda_{TCR} \Delta T \quad ; \quad \Delta F = \lambda_{ECS} \Delta T + \Delta Q. \tag{2}$$

This framework is similar to that used in previous studies [2]. Our λ_{ECS} is equivalent to a "climate response parameter" (called α in Gregory et. al.) that measures the overall feedback strength of the climate system. The transient parameter λ_{TCR}

measures the "climate resistance"[3], or the sum of λ_{ECS} and an ocean heat uptake efficacy κ, if it is assumed that $\Delta Q = \kappa \Delta T$.

We note that there are significant complications inherent in estimating both ECS and TCR from these transient single-forcing or historical simulations. Numerous studies (e.g. [14, 1, 5]) suggest that the net radiation lost to space is a function of the surface temperature pattern, itself largely related to geographical variations in ocean heat uptake. Winton et al[14] suggest that this may be simply incorporated into the global mean framework by multiplying ΔQ by an ocean heat uptake efficacy factor ϵ. This factor, which should not be confused with the ocean heat uptake efficiency κ, reflects the changing relationship between global mean ΔT and outgoing radiation [5] as the surface warming pattern evolves, and is shown[14] to be greater than unity in most models. Thus, our sensitivity estimates are likely to underestimate the "true" values, even when forcing efficacy is taken into account. We retain these definitions, however, for consistency with earlier literature estimating ECS and TCR from historical observations [10, 7, 13].

3. Efficacies

The efficacy of a particular driver is calculated from 5-member ensembles (6 in the "historical" case) forced only with that driver or collection of drivers. We calculate the TCR (from temperature and forcing changes relative to pre-industrial control) and ECS (from temperature, forcing, and ocean heat content changes) as described in the main text. Transient and equilibrium efficacies E_i are defined as the quotient of the TCR or ECS calculated from a model run with forcing i and the relevant previously published GISS-E2-R TCR and ECS values (1.4°C and 2.3°C respectively).

In the iRF case, where annual forcing time series are available, TCR and ECS are calculated by regressing ensemble-average decadal mean forcing or forcing minus ocean heat content change rate against ensemble-average temperature change. We assume that efficacies remain roughly constant in time over the historical period, an assumption bolstered by the high temporal correlation between ensemble average decadal mean temperature and forcing changes (with correlation coefficient over .99 for each single-forcing experiment). In the ERF case, we have only one decade available; hence efficacies are estimated using the quotient of temperature change and forcing and/or OHC uptake changes.

The uncertainty in the efficacies is estimated from individual members of the single-forcing ensembles (Figure S2). Confidence intervals on the sample mean are constructed using a student-t distribution with 4 degrees of freedom (5 in the case of the 6-member historical ensemble).

Table S1 lists the transient and equilibrium efficacies calculated from the GISS-E2-R single-forcing runs, along with uncertainties derived from the 5-member ensembles for each forcing.

We expect the transient and equilibrium efficacies of GHGs to be close to unity, as GHG forcing is dominated by CO_2 forcing. However, the GHG-only simulations also contain methane, CFCs, and other greenhouse gases, which may cause the efficacy to differ from one [4]. Additionally, different manifestations of internal variability, damped somewhat in the 5-member ensemble averages, result in GHG TCR and ECS values that depart from 1.4°C and 2.3°C, respectively. Finally, these deviations from published TCR/ECS values reflect the role of ocean heat uptake

	Instantaneous RF (iRF)		Effective RF (ERF)	
	$E_{transient}$	$E_{equilibrium}$	$E_{transient}$	$E_{equilibrium}$
AA	**1.55**(1.05,2.05)	**1.59**(1.33,1.84)	1.03(0.85,1.21)	0.95(0.85,1.06)
GHG	**1.17**(1.06,1.27)	1.06 (0.98,1.14)	0.99(0.90,1.09)	**0.85** (0.79,0.92)
LU	4.27 (-2.42,10.95)	1.27 (0.09,2.44)	2.25(-1.34,5.84)	1.64(-3.44,6.73)
Oz	**0.66**(0.34,0.98)	**0.52**(0.28,0.76)	**0.66** (0.38,0.94)	0.7(0.18,1.22)
Sl	1.68 (-1.27,4.63)	1.04 (0.36,1.73)	0.43(-0.61,1.46)	**0.22** (-0.41,0.86)
Vl	**0.61**(0.33,0.89)	0.7 (0.39,1.02)	0.56(-0.09,1.20)	0.73(-0.61,2.06)
historical	0.96 (0.80,1.12)	**0.78**(0.69,0.86)	**0.88** (0.83,0.92)	**0.76** (0.70,0.82)

TABLE S1. Transient and equilibrium efficacies (mean and 5-95% confidence intervals) calculated from instantaneous (iRF) and effective (ERF) radiative forcings. Values significantly different from unity are in bold.

efficacy: as the pattern of surface warming evolves, outgoing flux into space, and thus the rate at which heat must be taken up by the deep ocean, changes.

Figure 3 shows the GHG-only TCR and ECS estimated from decadal mean temperature, forcing, and OHC changes as a function of time. The spread determined by the individual ensemble members becomes smaller toward the end of the historical record as the forcing grows stronger, but the ECS and TCR ranges encompass the CO_2-only values. Rather than assume the efficacy of GHGs to be 1, we estimate GHG efficacy and its uncertainty from the ensemble.

4. Observations

Following previous work[10], we use the HadCRUT4 estimate[9] of the 2000–2009 temperature change relative to the base period (1860–1879), yielding $\Delta T = 0.75 \pm 0.02$ °C. For radiative forcing, we use IPCC best estimates and uncertainties of the effective radiative forcing (ERF) due to aerosols, solar and volcanic forcing, well-mixed greenhouse gases, ozone, and land use changes from 2000–2009 relative to the base period. There is some ambiguity in these forcing definitions[1], and for completeness we will investigate the implications of efficacies calculated using both iRF and ERF.

In Figure S4, we illustrate how existing TCR/ECS calculations using combined forcings are modified when efficacies (calculated in the GISS perfect model framework) are taken into account. We rely on three estimates[10, 13, 7], hereafter O13, S14, and LC14. Differences between our median estimates and confidence intervals and the previously reported estimates likely result from our treatment of forcing uncertainties. LC14 and O13 use the total radiative forcing in order to estimate sensitivities; here we attempt to break down this total forcing into a sum of contributions from individual forcing components, and treat uncertainties in these individual forcings as independent. The values of relevant quantities are shown in Table S2. In O13, present-day forcing estimates are defined as 2000–2009 averages with respect to the 1860–1879 base period. We estimate these forcings from the values and uncertainties given in IPCC AR5 WG1 Table AII.1.2, Table 8.SM.5,

[1]For example, the best-estimate 1750–2011 stratospherically adjusted RF and ERF values given by the IPCC are identical, except for aerosols (Table 8.SM.5 and Table 8.6).

Reference	ΔT	ΔQ	F_{GHG}	F_{AA}	F_{LU}	F_{Oz}	F_{Sl}	F_{Vl}
S14	0.68 ± 0.1	0.55 ± 0.27	2.47 ± 0.12	$-0.825(+0.3, -0.5)$	-0.085 ± 0.085	0.27 ± 0.14	0.03 ± 0.05	-0.125 ± 0.035
LC14	0.71 ± 0.15	0.36 ± 0.27	2.37 ± 0.57	$-0.68(+0.8, -0.1)$	-0.1025 ± 0.1	0.27 ± 0.21	0.03 ± 0.05	0.0 ± 0.04
O13	0.75 ± 0.1	0.65 ± 0.27	2.4 ± 0.28	-0.7 ± 0.7	-0.15 ± 0.1	0.28 ± 0.17	0.05 ± 0.05	-0.12 ± 0.04

TABLE S2. Observational estimates from three references: S14[13], LC14[7], and O13[10]. All forcings and OHC uptake rates are in units of watts per square meter; temperature ΔT is in K.

Percentile	S14 (E=1)	S14 (iRF)	S14 (ERF)	LC14 (E=1)	LC14 (iRF)	LC14 (ERF)	O13 (E=1)	O13 (iRF)	O13 (ERF)
TCR (50%)	1.4	1.8	1.6	1.3	1.4	1.5	1.3	1.7	1.6
5%	1.0	1.1	1.1	0.9	0.7	0.9	0.9	0.9	1.0
17%	1.2	1.4	1.3	1.0	1.0	1.1	1.0	1.1	1.2
83%	1.7	2.4	2.0	1.7	2.5	2.1	1.8	2.8	2.2
95%	2.0	3.3	2.4	2.5	5.1	3.3	2.3	5.3	3.1
ECS (50%)	2.1	3.4	3.4	1.5	1.8	2.1	2.0	2.6	3.1
5%	1.4	1.9	2.0	1.0	-3.1	1.1	1.1	-10.5	1.1
17%	1.7	2.4	2.5	1.2	1.2	1.5	1.4	1.4	1.9
83%	2.7	5.4	5.1	2.2	3.3	3.6	3.2	5.9	6.4
95%	3.4	9.3	8.0	3.6	7.7	7.2	5.4	16.0	15.0

TABLE S3. TCR and ECS percentiles calculated using observational estimates from three references: S14[13], LC14[7], and O13[10] assuming unit efficacy (E=1) and efficacies calculated from instantaneous (iRF) and effective (ERF) radiative forcing.

and Table 8.6. The IPCC report lists 2011 forcing uncertainties, which we scale by the ratio of 2009 forcing to 2011 forcing. We use ocean heat content uptake rate and temperature change values reported in the O13 supplementary material. The values used in LC14 are similar, although forcings are defined as 1995–2011 averages with respect to a base period of 1959–1882. We also use their different, lower values of ocean heat uptake rate and their stated temperature change. In S14, the responses to the sum of CMIP5 aerosol, ozone, and land use forcings are estimated using the differences between historical and the sum of "historicalNat" and "historicalGHG" simulations, with forcings and uncertainties determined from ACCMIP data.

In calculating TCR and ECS from these forcing, temperature, and ocean heat uptake values, we draw samples from normal distributions in the case where uncertainty is taken to be symmetric about the mean. Where the uncertainties are not symmetric about the mean (e.g. anthropogenic aerosol forcings) samples are drawn from a lognormal distribution.

Means, medians, and confidence intervals for TCR and ECS derived from these observational estimates are shown in Table S3.

4.1. **Incorporating estimated efficacies.** In order to take forcing efficacy into account, we scale each observed or simulated forcing ΔF_i by the calculated efficacy E_i. This modifies Eq (1) in the main text:

$$\sum_{i}^{n_{forcings}} E_i \Delta F_i = \lambda_{TCR} \Delta T \quad ; \quad \sum_{i}^{n_{forcings}} E_i \Delta F_i = \lambda_{ECS} \Delta T + \Delta Q. \tag{3}$$

In the perfect model framework, this results in a revision of the "best guess" TCR (calculated from the sum of single-forcing experiments) from 1.1°C to 1.4°C and of ECS from 1.6°C to 2.3°C (Figure 4).

References

[1] K. C. Armour, C. M. Bitz, and G. H. Roe. Time-varying climate sensitivity from regional feedbacks. *J. Clim.*, 26:4518–4534, 2013.

[2] J. M. Gregory, W. J. Ingram, M. A. Palmer, G. S. Jones, P. A. Stott, R. B. Thorpe, J. A. Lowe, T. C. Johns, and K. D. Williams. A new method for diagnosing radiative forcing and climate sensitivity. *Geophys. Res. Lett.*, 31, 2004.

[3] JM Gregory and PM Forster. Transient climate response estimated from radiative forcing and observed temperature change. *Journal of Geophysical Research: Atmospheres (1984–2012)*, 113(D23), 2008.

[4] J. E. Hansen, M. Sato, R. Ruedy, L. Nazarenko, A. Lacis, G. A. Schmidt, G. Russell, I. Aleinov, M. Bauer, S. Bauer, N. Bell, B. Cairns, V. Canuto, M. Chandler, Y. Cheng, A. Del Genio, G. Faluvegi, E. Fleming, A. Friend, T. Hall, C. Jackman, M. Kelley, N. Y. Kiang, D. Koch, J. Lean, J. Lerner, K. Lo, S. Menon, R. L. Miller, P. Minnis, T. Novakov, V. Oinas, Ja. Perlwitz, Ju. Perlwitz, D. Rind, A. Romanou, D. Shindell, P. Stone, S. Sun, N. Tausnev, D. Thresher, B. Wielicki, T. Wong, M. Yao, , and S. Zhang. Efficacy of climate forcings. *J. Geophys. Res.*, 110, 2005.

[5] Isaac M Held, Michael Winton, Ken Takahashi, Thomas Delworth, Fanrong Zeng, and Geoffrey K Vallis. Probing the fast and slow components of global warming by returning abruptly to preindustrial forcing. *Journal of Climate*, 23(9):2418–2427, 2010.

[6] J. T. Houghton, editor. *Climate Change: the IPCC Scientific Assessment*. Cambridge University Press, 2001. Report by the Intergovernmental Panel on Climate Change.

[7] Nicholas Lewis and Judith A. Curry. The implications for climate sensitivity of AR5 forcing and heat uptake estimates. *Clim. Dyn.*, sep 2014.

[8] R. L. Miller, G. A. Schmidt, L. S. Nazarenko, N. Tausnev, R. Ruedy, M. Kelley, K. K. Lo, I. Aleinov, M. Bauer, S. Bauer, R. Bleck, V. Canuto, Y. Cheng, T. L. Clune, A. Del Genio, G. Faluvegi, J. E. Hansen, R. J. Healy, N. Y. Kiang, D. Koch, A. A. Lacis, A. N. LeGrande, J. Lerner, S. Menon, V. Oinas, J. Perlwitz, M. J. Puma, D. Rind, A. Romanou, G. L. Russell, M. Sato, D. T. Shindell, S. Sun, K. Tsigaridis, N. Unger, A. Voulgarakis, M.-S. Yao, and J. Zhang. CMIP5 historical simulations (1850–2012) with GISS ModelE2. *J. Adv. Model. Earth Syst.*, 6:441–477, 2014.

[9] Colin P. Morice, John J. Kennedy, Nick A. Rayner, and Phil D. Jones. Quantifying uncertainties in global and regional temperature change using an ensemble of observational estimates: The HadCRUT4 data set. *J. Geophys. Res.*, 117(D8), 2012.

[10] A. Otto, F. E. L. Otto, O. Boucher, J. Church, G. Hegerl, P. M. Forster, N. P. Gillett, J. Gregory, G. C. Johnson, R. Knutti, N. Lewis, U. Lohmann, J. Marotzke, G. Myhre, D. T. Shindell, B. Stevens, and M. R. Allen. Energy budget constraints on climate response. *Nature Geosci.*, 6:415–416, 2013.

[11] Matthew D Palmer, Douglas J McNeall, and Nick J Dunstone. Importance of the deep ocean for estimating decadal changes in earth's radiation balance. *Geophysical Research Letters*, 38(13), 2011.

[12] Gavin A. Schmidt, Max Kelley, Larissa Nazarenko, Reto Ruedy, Gary L. Russell, Igor Aleinov, Mike Bauer, Susanne Bauer, M. K. Bhat, Rainer Bleck, Vittorio Canuto, Y. Chen, Ye Cheng, Thomas L. Clune, Anthony Del Genio, R. de Fainchtein, Greg Faluvegi, James E. Hansen, Richard J. Healy, Nancy Y. Kiang, Dorothy Koch, Andy A. Lacis, Allegra N. LeGrande, Jean Lerner, Ken K. Lo, Elaine E. Matthews, Surabi Menon, Ron L. Miller, Valdar Oinas, A. O. Oloso, Jan Perlwitz, Michael J. Puma, William M. Putman, David Rind, Anastasia Romanou, Makiko Sato, Drew T. Shindell, Shan Sun, R.A. Syed, Nick Tausnev, K. Tsigaridis, Nadine Unger, A. Voulgarakis, Mao-Sung Yao, and Jinlun Zhang. Configuration and assessment of the GISS ModelE2 contributions to the CMIP5 archive. *J. Adv. Model. Earth Syst.*, 6:141–184, 2014.

[13] Drew T. Shindell. Inhomogeneous forcing and transient climate sensitivity. *Nature Climate Change*, 4(4):274–277, mar 2014.

[14] Michael Winton, Ken Takahashi, and Isaac M Held. Importance of ocean heat uptake efficacy to transient climate change. *Journal of Climate*, 23(9):2333–2344, 2010.

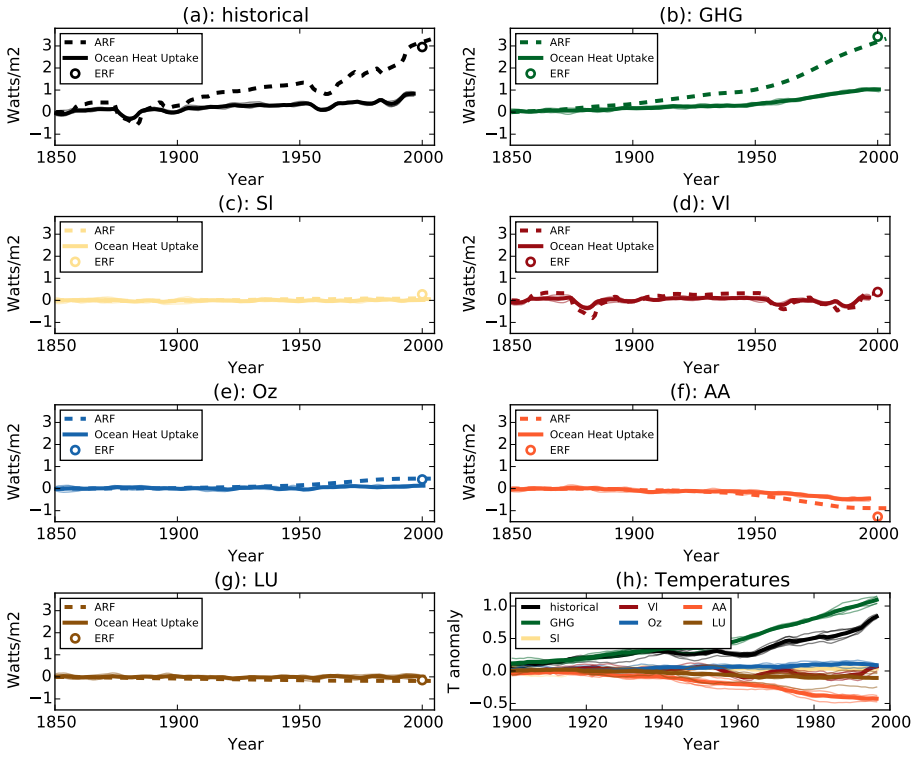

FIGURE S1. **Forcing, ocean heat uptake, and temperature changes.**(a-g): Ensemble-average instantaneous radiative forcings and ocean heat uptake rates (thick lines) and individual ensemble members (thin) for GISS-E2-R single-forcing experiments. All quantities are 10-year running means. Dots represent year-2000 effective radiative forcings (ERF). (h): Ensemble-average temperature anomalies (relative to 1850) for each single-forcing simulation.

NASA GODDARD INSTITUTE FOR SPACE STUDIES AND DEPARTMENT OF APPLIED MATHEMATICS AND APPLIED PHYSICS, COLUMBIA UNIVERSITY, NEW YORK, NY 10025
E-mail address: kate.marvel@nasa.gov

NASA GODDARD INSTITUTE FOR SPACE STUDIES NEW YORK, NY 10025
E-mail address: gavin.a.schmidt@nasa.gov

NASA GODDARD INSTITUTE FOR SPACE STUDIES NEW YORK, NY 10025
E-mail address: ron.l.miller@nasa.gov

NASA GODDARD INSTITUTE FOR SPACE STUDIES AND CENTER FOR CLIMATE SYSTEMS RESEARCH, COLUMBIA UNIVERSITY, NEW YORK, NY 10025
E-mail address: larissa.s.nazarenko@nasa.gov

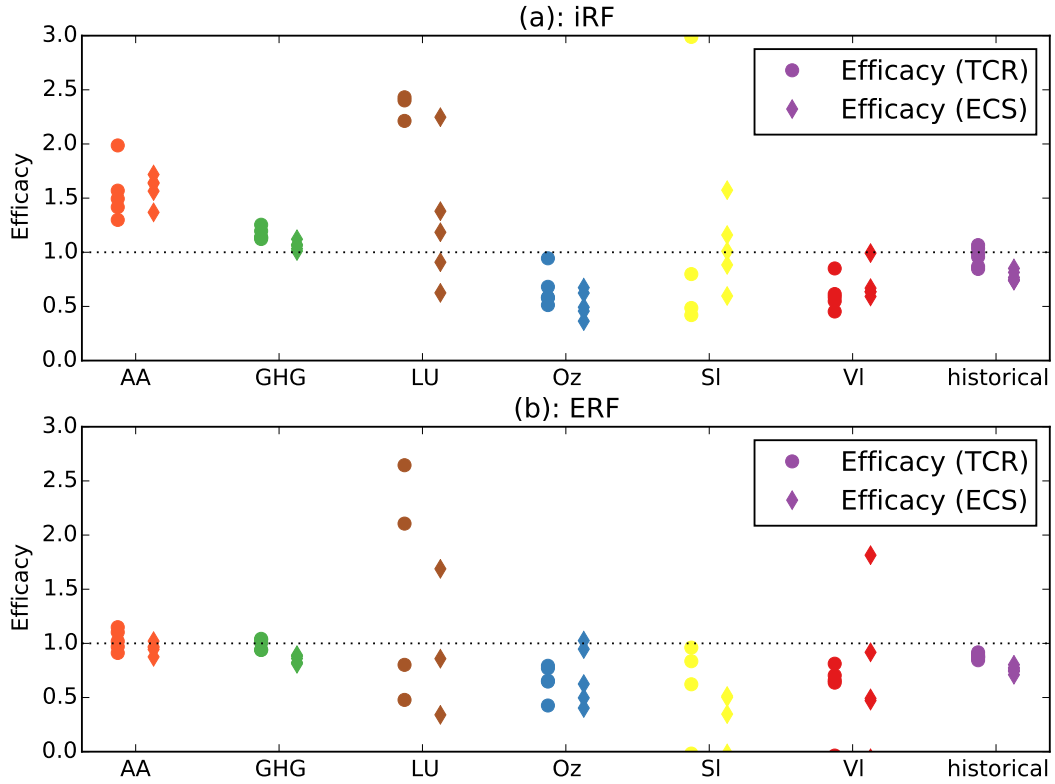

FIGURE S2. **Transient (circles) and equilibrium efficacies calculated for each ensemble member in the single-forcing and historical ensembles.** Efficacies are calculated using (a) iRF and (b) ERF.

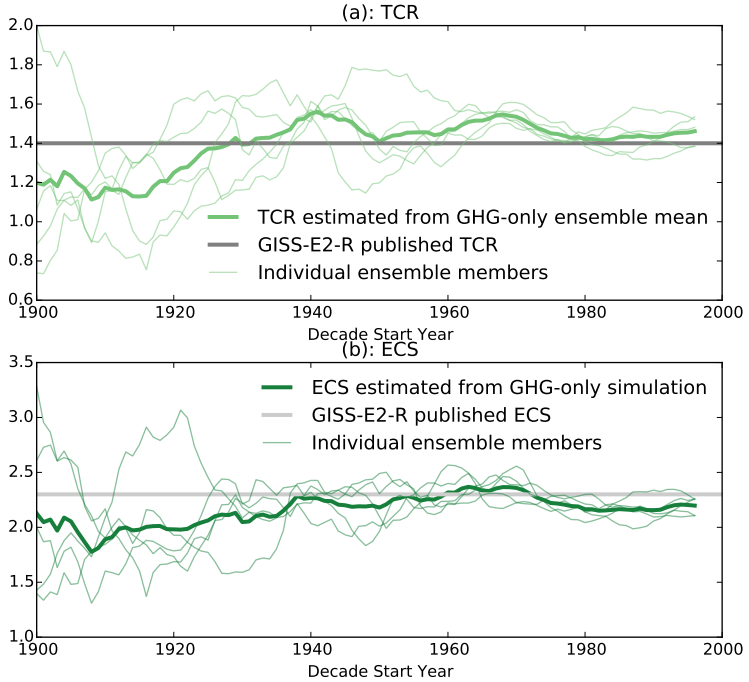

FIGURE S3. **Decadal variation in sensitivity estimates.** (a): Transient and (b): equilibrium sensitivities estimated from 10-year means of temperature and forcing change and OHC change (in the equilibrium case) relative to pre-industrial control values.

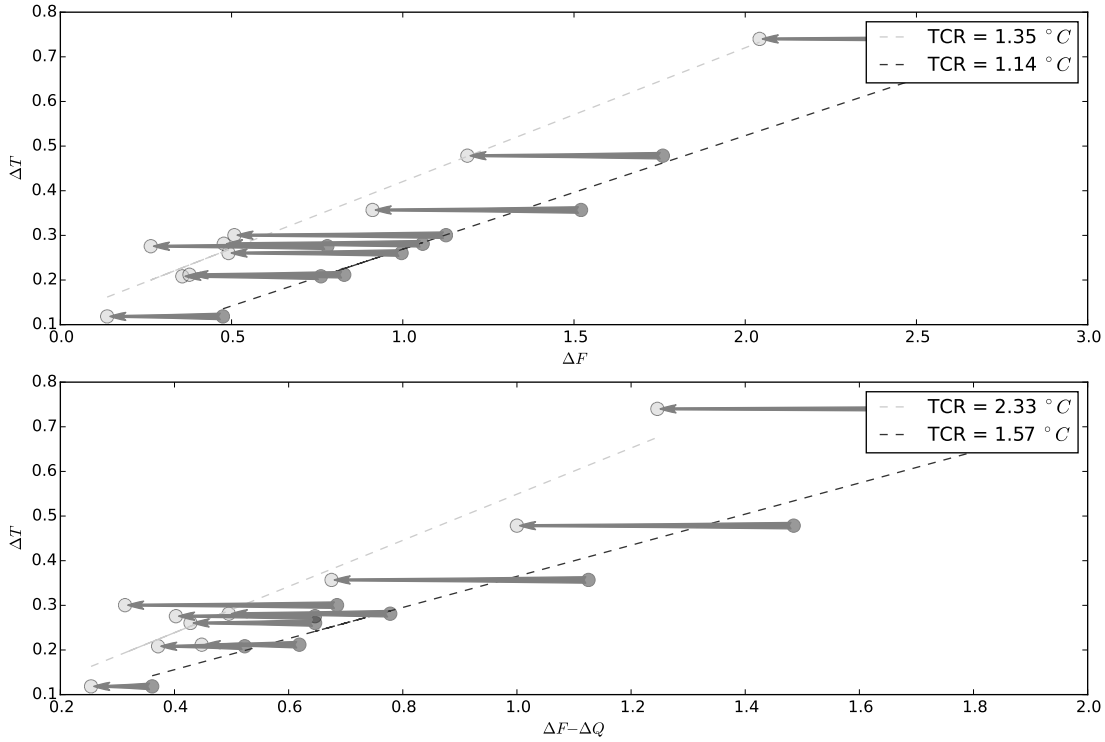

FIGURE S4. **Model historical sensitivies when efficacies are taken into account** (a): Transient and (b): equilibrium sensitivities estimated from 10-year means without (dark gray) and with (light gray) efficacy scaling.